



ELSEVIER

Applied Surface Science 168 (2000) 208–214

applied
surface science

www.elsevier.nl/locate/apsusc

Superconducting and electro-optical thin films prepared by pulsed laser deposition technique

J. Schubert^{a,*}, M. Siegert^a, M. Fardmanesh^c, W. Zander^a,
M. Prömpers^a, Ch. Buchal^a, Judit Lisoni^a, C.H. Lei^b

^aInstitut für Schicht- und Ionentechnik, Forschungszentrum Jülich GmbH, 52425 Jülich, Germany

^bInstitut für Festkörperforschung, Forschungszentrum Jülich GmbH, 52425 Jülich, Germany

^cOn leave from Electrical and Electronics Engineering Department, Bilkent University, Ankara, Turkey

Abstract

The pulsed laser deposition (PLD) technique is an excellent method to prepare single crystalline complex oxide thin films. We have successfully grown films for the use in HTS SQUID-devices as well as for thin film optical waveguides. The Josephson junction used in the HTS SQUIDs is formed by a step edge type grain boundary junction. The step preparation is a very critical process in the SQUID preparation to achieve reproducible low $1/f$ noise devices. We have established a new ion beam etching process to achieve clean and steep edges in $\text{LaAlO}_3(1\ 0\ 0)$ substrates. The $1/f$ noise of SQUIDs prepared with the new method is drastically reduced. In the process of developing thin film electro-optical waveguide modulators we investigated the influence of different substrates on the optical and structural properties of epitaxial BaTiO_3 thin films. These films are grown on $\text{MgO}(1\ 0\ 0)$, $\text{MgAl}_2\text{O}_4(1\ 0\ 0)$, $\text{SrTiO}_3(1\ 0\ 0)$ and MgO buffered $\text{Al}_2\text{O}_3(1\ \bar{1}\ 0\ 2)$ substrates. The waveguide losses and the refractive indices were measured with a prism coupling setup. The optical data are correlated to the results of Rutherford backscattering spectrometry/ion channeling (RBS/C), X-ray diffraction (XRD), atomic force microscopy (AFM) and transmission electron microscopy (TEM). The dielectric constant, the ferroelectric hysteresis loop and the transition temperature (ferroelectric to paraelectric state) of the BaTiO_3 thin films are measured. © 2000 Elsevier Science B.V. All rights reserved.

Keywords: Pulsed laser deposition; rf-SQUID; High temperature superconductor; Optical waveguide

1. Introduction

Pulsed laser deposition (PLD) is a successful thin film deposition method for the preparation of epitaxial oxide films on different single crystalline substrates [1]. Several deposition methods like MOCVD [2], MBE [3,4] and rf magnetron sputtering [5] have been used to deposit HTS-material as $\text{YBa}_2\text{Cu}_3\text{O}_{7-x}$, ferro-

electric BaTiO_3 and other perovskite thin films on many different substrates. The advantage of PLD is the stoichiometric transfer of complex target materials to the substrate, which can be maintained at a high temperature in a reactive atmosphere. Many new devices may be formed using such high quality single crystalline oxide thin films. Low noise high temperature superconductor (HTS) rf-SQUIDs prepared from $\text{YBa}_2\text{Cu}_3\text{O}_{7-x}$, which are used in the nondestructive evaluation of defects in air plane wheels, are just one example for these devices [6]. The improvement of the fabrication yield of these SQUIDs in order to achieve

* Corresponding author. Tel.: +49-2461-616379;

fax: +49-2461-614673.

E-mail address: j.schubert@fz-juelich.de (J. Schubert).

reproducible low $1/f$ noise performance is a big challenge. We will demonstrate a new ion beam etching method to obtain clean steep steps in $\text{LaAlO}_3(1\ 0\ 0)$ which improve the yield of low noise SQUIDs drastically. Furthermore it has been shown, that BaTiO_3 thin films of high transparency and good structural properties can be grown on $\text{MgO}(1\ 0\ 0)$ [7]. Their high quality offers the possibility to use the films for optical waveguides and devices. The large electro-optic coefficients of BaTiO_3 makes this material especially suited for an electro-optical thin film modulator [8]. In this study we have investigated the influence of different substrates on the structural and optical properties of BaTiO_3 thin films.

2. Experimental

2.1. HTS-SQUID preparation and characterization

Our PLD system employs a Lambda Physics LPX 305 KrF excimer laser (248 nm, 20 ns, approx. 1 J/pulse, up to 50 Hz) [9]. The laser beam is focused by a cylindrical lens ($f = 400$ mm), resulting in an energy density of more than $2.5\ \text{J}/\text{cm}^2$ at the target. The cylindrical target consists of single phase $\text{YBa}_2\text{Cu}_3\text{O}_{7-x}$ powder which has been pressed and sintered. The SQUIDs are prepared from a 200 nm thick epitaxial single crystalline $\text{YBa}_2\text{Cu}_3\text{O}_{7-x}$ film

prepared by PLD on a single crystalline $\text{LaAlO}_3(1\ 0\ 0)$ substrate $10\ \text{mm} \times 10\ \text{mm} \times 1\ \text{mm}$. The typical deposition temperature for the $\text{YBa}_2\text{Cu}_3\text{O}_{7-x}$ thin film was 780°C in an oxygen ambient of 1 mbar pure oxygen. These films show $T_c > 89\ \text{K}$, $j_c(T = 77\ \text{K}) > 3 \times 10^6\ \text{A}/\text{cm}^2$ and a crystalline perfection measured by the minimum yield value $\chi_{\min} < 4\%$ in a RBS/channeling analysis. In our work we use “rf-washer-SQUIDs” described elsewhere [10]. The rf-SQUIDs have a washer size of 3.5 mm in diameter, SQUID holes of $150\ \mu\text{m} \times 150\ \mu\text{m}$ resulting in a SQUID-inductivity of 250 pH and a junction line width of 1–5 μm .

The $\text{YBa}_2\text{Cu}_3\text{O}_{7-x}$, thin film was patterned by wet chemical etching [11] using a resist mask defined by conventional photolithography. The step formation in the substrate of the 270 nm deep trench was performed by an ion beam etching procedure using a resist mask defined by photolithography. The dimensions of the trench prepared in the substrates is $8\ \mu\text{m} \times 100\ \mu\text{m}$. The standard method to prepare the trenches in the substrate is to use an incident Ar^+ -ion beam ($U = 400\ \text{V}$, $I = 80\ \text{mA}$) parallel to the normal of the substrate surface with a rotating substrate. The typical spread in the $1/f$ noise spectra of six SQUIDs prepared in one batch, on steps prepared with this process is seen in Fig. 1.

All of these SQUIDs show a white noise level lower than $20\ \mu\Phi$. at frequencies higher than 5 kHz. A large

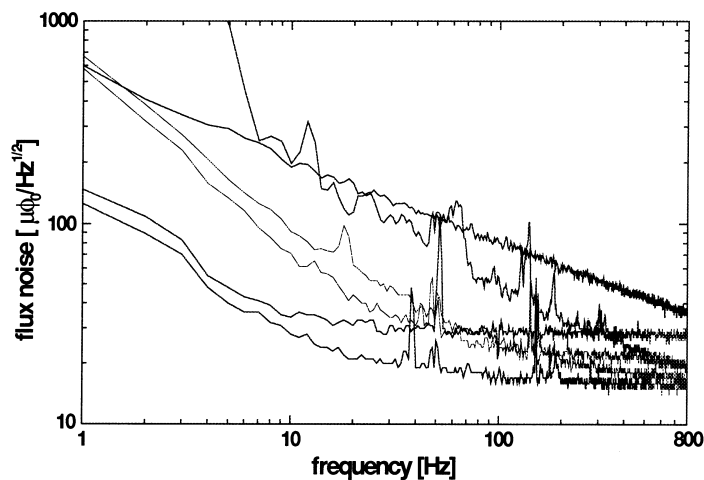


Fig. 1. Noise spectra of six rf-washer SQUIDs prepared in one fabrication cycle using the standard step edge ion-beam etching process with vertical incidence.

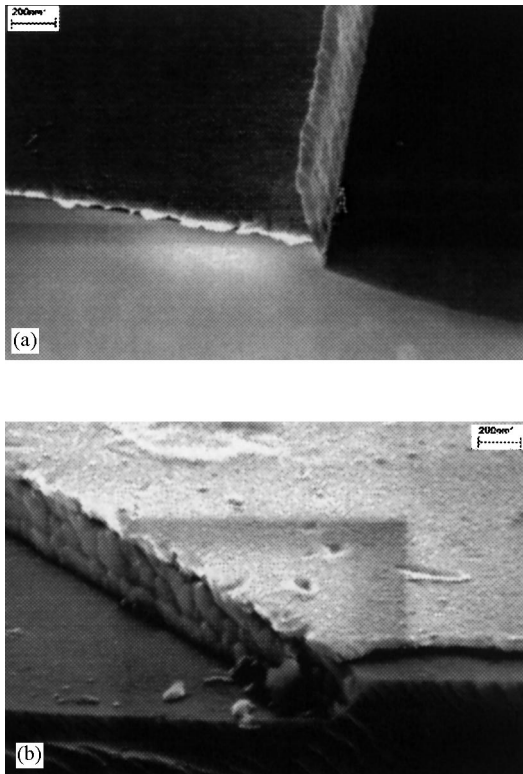


Fig. 2. (a) Redeposited material formed by amorphous substrate material covering the edge; (b) clean step in a $\text{LaAlO}_3(100)$ substrate formed by the new IBE-method.

spread in the noise behavior in the low frequency regime is clearly seen. The reason for this noise figure is found in a fence of redeposited material grown during the ion beam etching process. This fence which is seen in Fig. 2a consists of amorphous substrate material. The whole trench formed during the etching process is covered by this amorphous layer of LaAlO_3 .

These results indicate that the IBE-process is critical for the junction formation and the performance of the rf-SQUIDs. Hence, we have investigated the IBE-process. The goal of our investigation was to establish an IBE-process which produces a steep clean step angle $<70^\circ$ as a base for step edge junctions in order to reduce the spread in the $1/f$ -noise of our rf-SQUIDs. Using a rotating substrate and an angle of incidence of 45° of the ion beam with regard to the surface of the substrate we achieve a clean step with a step angle $<50^\circ$ (process 1) [12]. An alternative method is to align the direction of a fixed ion beam parallel to the

long edge of the trench forming photoresist mask (process 2). Using the “process 2” we have found an improvement in the noise behavior of the SQUIDs. The best results were obtained using a combination of the two ion beam etching processes. At first using the “process 2”, a trench is formed by a fixed ion beam which is adjusted parallel to the long edge of the trench forming edges of the photoresist. So, a 270 nm deep trench is formed by a fixed Ar^+ -beam using 500 eV beam energy and a current of 0.5 mA/cm^2 . The incident angle of the beam was 40° with respect to the substrate surface. Then, the “process 1” was used to clean the edge surface using a rotating substrate with a beam energy of 300 eV, current density of 0.5 mA/cm^2 and an angle of incidence of 45° . The noise figures of SQUIDs prepared on these steps are seen in Fig. 3. The white noise level of these SQUIDs in comparison to the SQUIDs made with the standard process is not changed. A drastic improvement in the low frequency noise performance is visible and the noise spread is also reduced. The noise level at 10 Hz is approx. $30 \mu\Phi$. In conclusion, using the two IBE-processes the $1/f$ noise as well as the reproducibility of step edge junction rf-SQUIDs was improved dramatically.

2.2. Electro-optical BaTiO_3 thin films

BaTiO_3 thin films were prepared on different single crystalline substrates. The cylindrical target for the PLD-process consists of single phase BaTiO_3 powder which has been pressed and sintered. The structural and optical parameters of these substrates are listed in Table 1. The optimized deposition conditions are very similar for all substrate materials. First the deposition chamber was evacuated to 8×10^{-4} mbar by a turbomolecular pump. Then an atmosphere of 2×10^{-3} mbar of oxygen was introduced and within 5 min the substrates were heated to the deposition temperature by a SiC heater. For MgO and SrTiO_3 substrates the heater temperature was approx. 1000°C . For MgAl_2O_4 and MgO buffered Al_2O_3 , a slightly higher heater temperature of approx. 1050°C was needed. The target-substrate distance was 4 cm. The repetition rate of the excimer laser was kept at 10 Hz. The growth rate was as high as 0.4 nm/pulse, resulting in very short deposition times of approx. 250 s for a 1 μm thick BaTiO_3 film. Directly after the deposition

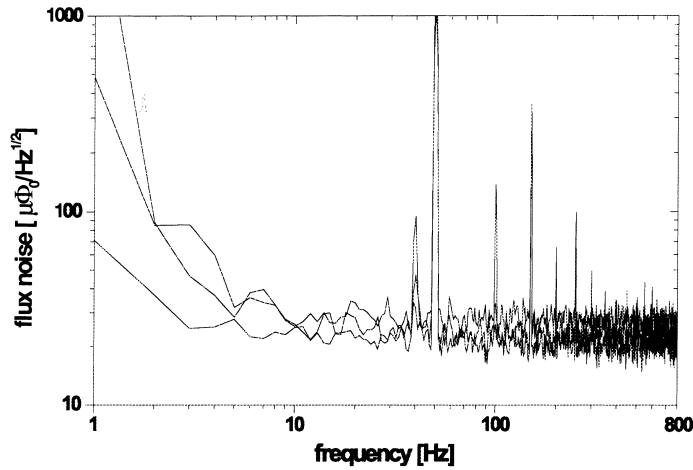


Fig. 3. Noise spectra of SQUIDs prepared with the combinational IBE method for the preparation of the step in the substrate.

the heater was switched off and the chamber was flooded with oxygen up to atmospheric pressure. After 5 min of cooling down the samples were removed from the chamber. With these parameters we obtained epitaxial *c*-axis oriented BaTiO₃ films on all substrates, except on MgO buffered Al₂O₃, where we were able to obtain *a*-axis oriented films at 1050°C. The low refractive index of Al₂O₃ would favor a direct deposition of BaTiO₃. However, under our experimental conditions, only polycrystalline films were obtained. A MgO buffer layer on Al₂O₃ promotes the epitaxial growth of BaTiO₃ [13].

As an example a RBS/C measurement of a 562 nm thick BaTiO₃ film grown on SrTiO₃(1 0 0) is shown in Fig. 4. The Ba:Ti ratio is 1:1 within the experimental accuracy of RBS (1 at.%). The value of the minimum

yield χ_{\min} of 0.5% measured at the Ba-signal is comparable to those observed for BaTiO₃ single crystals. A summary of the RBS/C, XRD, AFM and waveguide loss measurement results of BaTiO₃ films is shown in Table 2. SrTiO₃ and BaTiO₃ belong to the perovskite crystal family. In combination with the small misfit (<3.3%) (Table 1), this leads to the superior structural properties of the BaTiO₃ films grown on SrTiO₃. Nevertheless, the high refractive index of SrTiO₃ prevents the formation of waveguides. A HRTEM micrograph is shown in Fig. 5a. The interface between BaTiO₃ and SrTiO₃ is atomically flat. Only a low density of misfit dislocations could be observed.

For the other substrates, the HR-TEM micrographs display similar growth patterns. The interfaces are characterized by a higher number of misfit disloca-

Table 1
Structural and optical parameters of BaTiO₃ and relevant substrate materials^a

	<i>a</i> ^b (Å)	<i>n</i> ^c	α^d (10 ⁻⁶ /K)	<i>m</i> ^e (%)
BaTiO ₃	3.993/4.035	2.41/2.36	10.1–11.5	–
MgO	4.213	1.73	10.5	–5.22/–4.23
SrTiO ₃	3.905	2.39	10.3	2.25/3.33
MgAl ₂ O ₄	8.10 (2 × 4.05)	1.73	5.9	1.41/–0.37
Al ₂ O ₃	4.759/5.130	1.76	5.0–5.8	16.41/–15.53

^a For Al₂O₃, the lattice parameters of the pseudo cubic R-cut plane are given. Since BaTiO₃ is tetragonal at room temperature, first the *a*–*b* and second the *c* lattice parameters are noted.

^b Lattice parameter.

^c Refractive index at $\lambda = 632.8$ nm.

^d Thermal expansion coefficient at *T* = 293 K.

^e $(a_{\text{film}} - a_{\text{substrate}})/a_{\text{substrate}}$: the lattice mismatch.

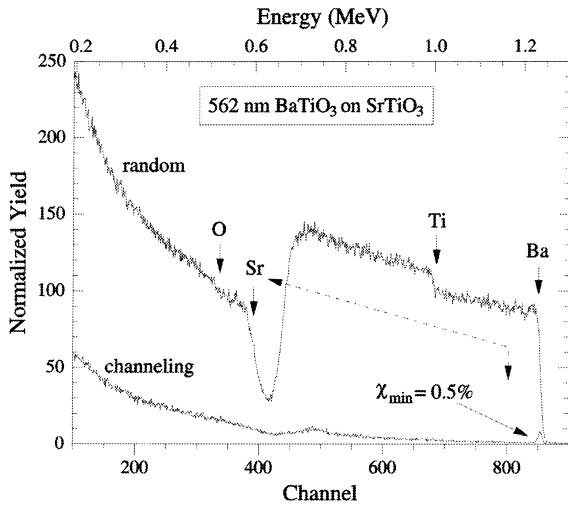


Fig. 4. RBS/channeling measurement of a BaTiO₃ thin film grown on SrTiO₃(1 0 0).

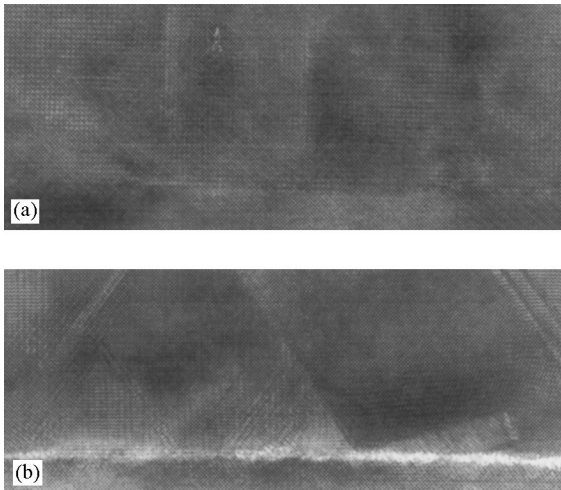


Fig. 5. High resolution TEM cross-sections of BaTiO₃ films deposited on (a) SrTiO₃ and (b) MgAl₂O₄ substrates.

Table 2
Structural and optical parameters of BaTiO₃ thin films grown on different substrate materials

Substrate	χ_{\min}^a (%)	$\Delta\omega$ (002) ^b (°)	σ^c (nm)	L^d (dB/cm)	Reference
SrTiO ₃	<1	0.35	<1	–	–
MgO	1	0.42	<1	3	[7]
MgAl ₂ O ₄	3.5	0.50	1	6	–
MgO–Al ₂ O ₃	5	0.64	1	8	[13]

^a RBS/C minimum yield for 1.4 MeV He⁺ ions.

^b Rocking curve width for the (0 0 2) reflex of BaTiO₃.

^c The rms surface roughness measured with an AFM on 3 $\mu\text{m} \times 3 \mu\text{m}$.

^d Optical losses of a planar waveguide at $\lambda = 632.8 \text{ nm}$.

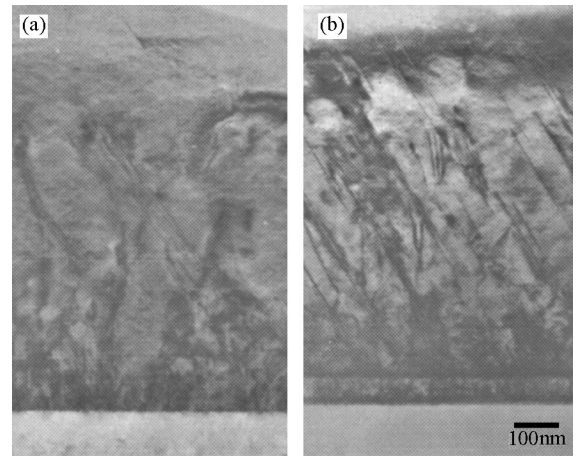


Fig. 6. TEM cross sections of BaTiO₃ films deposited (a) on MgO and (b) on MgO buffered Al₂O₃ substrates. Both films show a high density of misfit dislocations near the interfaces.

tions with respect to SrTiO₃. On MgAl₂O₄ also twins were visible (see Fig. 5b).

A TEM cross sectional image of a BaTiO₃ film grown on MgO(1 0 0) is shown in Fig. 6a. Near the interface between BaTiO₃ and MgO, there is a high density of misfit dislocations. However, only a few of them propagate through the film up to the surface. Films on MgO buffered Al₂O₃ and on MgAl₂O₄ showed a somewhat higher number of defects (see Fig. 6b). TEM diffraction analysis of the samples confirmed the cubic-to-cubic orientation relationship between BaTiO₃ and the different substrates, also corroborated by a X-ray φ -scan.

Because the thermal expansion coefficient of Al₂O₃ and MgAl₂O₄ is lower than that of BaTiO₃, the thickness of crack free films is limited to about

450 nm. Thicker films show a micro crack pattern, which becomes visible under an optical microscope. One micrometer thick BaTiO₃ films on MgO and 440 nm thick films on MgO buffered Al₂O₃ and on MgAl₂O₄ were used for optical waveguides.

The lowest waveguide losses of 3 dB/cm were obtained on MgO substrates. This is correlated to the better structural properties in comparison to films on MgO buffered Al₂O₃ (8 dB/cm). However, one should note, that the waveguide thickness has a strong influence on the transmission losses. According to [14], the losses due to surface scattering α_{sc} can be estimated by

$$\alpha_{sc} = \left(\frac{4\pi\sigma}{\lambda}\right)^2 \times \left(\frac{f(\varphi)}{t}\right) \quad (1)$$

where σ is the rms surface roughness, λ the wavelength, $f(\varphi)$ a geometric parameter associated with the angle of reflection φ and t the waveguide thickness. The scattering losses decrease by 50% if the film thickness is increased from 500 to 1 μ m. Changing the wavelength from 632.8 to 1.55 μ m decreases these losses by more than 80%.

Electrical characterizations were performed using an interdigital electrode structure for capacitance measurements. In a temperature dependent measurement the transition from the ferro- to paraelectric phase was observed. The transition temperature of about 200°C is higher than that of single crystalline BaTiO₃ bulk material (120°C) which is attributed to the presence of stress in the single crystalline thin films [15]. On MgO(1 0 0) substrates the dielectric constant of the BaTiO₃ thin films has values around $\epsilon = 1000 \pm 100$. On SrTiO₃(1 0 0) these values are much higher (around $\epsilon = 3000 \pm 300$). The large variation in the values on different substrates is attributed to the difference in the crystalline perfection of the films. Further investigations of the dielectric constant, remanent polarization and coercitive field in this BaTiO₃ thin films are in progress.

3. Summary

The PLD was successfully used to prepare high quality epitaxial superconducting and BaTiO₃ thin films for use in optical waveguide applications.

SQUID-performance of rf-washer SQUIDs could be improved by establishing a new ion beam etching method for the preparation of the step in the substrate which prevents redeposited material at the trench steadily. Single crystalline BaTiO₃ films were grown on different substrates. The best structural properties were obtained on SrTiO₃. The optical losses of films on MgO, on MgAl₂O₄ and on MgO buffered Al₂O₃ where 3, 6 and 8 dB/cm for $\lambda = 632.8$ nm, but it is expected that these values can be reduced significantly by changing to the telecommunication wavelength of 1.55 μ m. The relative dielectric constant of the films is depending on the substrate and the transition from the ferroelectric to the paraelectric state is observed at temperatures higher than 120°C (Curie temperature for bulk single crystals).

Acknowledgements

The authors gratefully acknowledge the support from the Tandetron facility and the staff of the IFF of the Forschungszentrum Jülich. This work has been supported partly by the ESPRIT Long Term Research Project No. 31838 SCOOP (Silicon Compatible Optoelectronics) and the German government founded research project No. 13N7327 “SQUID2000”.

References

- [1] K.L. Saenger, *Process. Adv. Mat.* 2 (1993) 1.
- [2] D.M. Gill, B.A. Block, C.W. Conrad, B.W. Wessels, S.T. Ho, *Appl. Phys. Lett.* 69 (1996) 2968.
- [3] F.J. Walker, R.A. McKee, *Appl. Phys. Lett.* 65 (1994) 1495.
- [4] R.A. McKee, F.J. Walker, M.F. Chisholm, *Phys. Rev. Lett.* 81 (1998) 3014.
- [5] P. Barrios, H.K. Kim, *Appl. Phys. Lett.* 73 (1998) 1017.
- [6] A.I. Braginski, H.-J. Krause, J. Vrba, SQUID magnetometers, in: M.H. Francombe (Ed.), *Superconducting Film Devices, Handbook of Thin Film Devices*, Vol. 3, Academic Press, San Diego, 2000, pp. 149–225.
- [7] L. Beckers, J. Schubert, W. Zander, J. Ziesmann, A. Eckau, P. Leinenbach, Ch. Buchal, *J. Appl. Phys.* 83 (1998) 3305.
- [8] M. Zgonik, P. Bernasconi, M. Duelli, R. Schlessler, P. Günter, M.H. Garrett, D. Rytz, Y. Zhu, X. Wu, *Phys. Rev. B* 50 (1994) 5941.

- [9] B. Stritzker, J. Schubert, U. Poppe, W. Zander, U. Krüger, A. Lubig, Ch. Buchal, *J. Less-Common Met.* 164–165 (1990) 279.
- [10] Y. Zhang, M. Mück, K. Herrmann, J. Schubert, W. Zander, A.I. Braginski, C. Heiden, *Appl. Phys. Lett.* 60 (1992) 645.
- [11] F.-M. Kamm, A. Plettl, P. Ziemann, *Supercond. Sci. Technol.* 12 (11) (1998) 1397–1400.
- [12] K. Hermann, G. Kunkel, M. Siegel, J. Schubert, W. Zander, A.I. Braginski, C.L. Jia, B. Kabius, K. Urban, *J. Appl. Phys.* 78 (1995) 1131.
- [13] J.G. Lisoni, M. Siegert, C.H. Lei, J. Schubert, W. Zander, Ch. Buchal, Thin films for optical waveguide devices, *Mat. Res. Soc. Symp. Proc.*, 2000, vol. 597, in press.
- [14] B.W. Wessels, *J. Crystal Growth* 195 (1998) 706.
- [15] S.B. Desu, *J. Electrochem. Soc.* 140 (1993) 2981.